J Antimicrob Chemother 2015; **70**: 1367–1380
doi:10.1093/jac/dku545 Advance Access publication 27 January 2015

Journal of Antimicrobial Chemotherapy

ST-246 is a key antiviral to inhibit the viral F13L phospholipase, one of the essential proteins for orthopoxvirus wrapping

Sophie Duraffour[1]*, María M. Lorenzo[2], Gudrun Zöller[3], Dimitri Topalis[1], Doug Grosenbach[4], Dennis E. Hruby[4], Graciela Andrei[1], Rafael Blasco[2], Hermann Meyer[3] and Robert Snoeck[1]

[1]*Rega Institute, Laboratory of Virology and Chemotherapy, KU Leuven, Leuven, Belgium;* [2]*Departamento de Biotecnología, INIA, Madrid, Spain;* [3]*Bundeswehr Institute of Microbiology, Munich, Germany;* [4]*SIGA Technologies Inc., Corvallis, OR, USA*

*Corresponding author. Tel: +3216337395; Fax: +3216337340; E-mail: sophie.duraffour@rega.kuleuven.be

Received 20 October 2014; returned 24 November 2014; revised 1 December 2014; accepted 2 December 2014

Objectives: ST-246 is one of the key antivirals being developed to fight orthopoxvirus (OPV) infections. Its exact mode of action is not completely understood, but it has been reported to interfere with the wrapping of infectious virions, for which F13L (peripheral membrane protein) and B5R (type I glycoprotein) are required. Here we monitored the appearance of ST-246 resistance to identify its molecular target.

Methods: Vaccinia virus (VACV), cowpox virus (CPXV) and camelpox virus (CMLV) with reduced susceptibility to ST-246 were selected in cell culture and further characterized by antiviral assays and immunofluorescence. A panel of recombinant OPVs was engineered and a putative 3D model of F13L coupled with molecular docking was used to visualize drug–target interaction. The *F13L* gene of 65 CPXVs was sequenced to investigate F13L amino acid heterogeneity.

Results: Amino acid substitutions or insertions were found in the *F13L* gene of six drug-resistant OPVs and production of four F13L-recombinant viruses confirmed their role(s) in the occurrence of ST-246 resistance. F13L, but not B5R, knockout OPVs showed resistance to ST-246. ST-246 treatment of WT OPVs delocalized F13L- and B5R-encoded proteins and blocked virus wrapping. Putative modelling of F13L and ST-246 revealed a probable pocket into which ST-246 penetrates. None of the identified amino acid changes occurred naturally among newly sequenced or NCBI-derived OPV F13L sequences.

Conclusions: Besides demonstrating that F13L is a direct target of ST-246, we also identified novel F13L residues involved in the interaction with ST-246. These findings are important for ST-246 use in the clinic and crucial for future drug-resistance surveillance programmes.

Keywords: poxvirus, drug resistance, mechanisms of action, antivirals, vaccinia virus

Introduction

ST-246 (Tecovirimat®) is a small molecule that specifically inhibits viruses belonging to the *Orthopoxvirus* (OPV) genus, which includes in particular variola virus (VARV), the causative agent of smallpox, monkeypox virus, cowpox virus (CPXV), vaccinia virus (VACV) and camelpox virus (CMLV). Renewed interest in OPV-related diseases has resulted mainly from the bioterrorist threat posed by the potential release of VARV. Nowadays, other OPVs are of concern in relation to both human and/or animal health,[1] and this has been highlighted by several reports of outbreaks of cowpox in Eurasia,[2–5] vaccinia in Brazil (i.e. Cantagalo virus)[6,7] and India (i.e. buffalopox virus),[8] monkeypox in Africa[9] and camelpox in the Middle East.[10] Also, the potential risk of laboratory-acquired infections should not be underestimated,[1,11–14] and neither should the unexpected discovery of undocumented smallpox vials stored in an unsecure safety environment in a laboratory.[15] Today, with regard to the emergence of pathogenic viruses such as Ebola, dengue, chikungunya and Middle East respiratory syndrome coronavirus, the significant public health concern posed by OPVs should not be ignored.[1,16–18]

Described for the first time in 2005 by Yang *et al.*,[19] ST-246 has been shown to be highly active *in vitro* (nanomolar range) and *in vivo* against OPVs.[20–27] Various animal models of OPV diseases have been used, such as mice, rabbits, ground squirrels, prairie dogs and non-human primates.[20,25,27–30] The compound is orally available, safe and well tolerated in healthy human volunteers and is currently in clinical development for the treatment of

OPV-related infections, including smallpox, in case this disease should reappear in the human population.[28,31–34] ST-246 might be beneficial as post-exposure therapy and as an adjunct to smallpox vaccination.[35] Under its investigational new drug status, ST-246 has been used in humans in the treatment of life-threatening VACV-related diseases, with the concomitant administration of other therapeutic agents.[36,37]

ST-246 has been shown to impede the envelopment of virions and the egress of enveloped viruses from the infected cell.[19,38] One mutant of CPXV strain Brighton (CPXV-BR) resistant to ST-246 has been described,[19] and a G277C amino acid change in F13L was found to be responsible for the drug-resistant phenotype [800-fold increase in 50% effective concentration (EC_{50}); 0.05 μM (WT) versus 40 μM (drug resistant)]. F13L is one of the pivotal proteins required for the production of enveloped virions. During OPV morphogenesis, intracellular mature viruses are formed (for review, see Smith[39]). These virions can then exit the cell after cell lysis and/or pursue their morphogenesis by becoming wrapped in virus-modified *trans*-Golgi or endosome membranes to produce enveloped viruses [EVs; these may remain associated with the infected cell as cell-associated enveloped virus (CEV) or be released into the extracellular medium as extracellular enveloped virus (EEV)]. F13L is one of the viral proteins anchored in these wrapping membranes. It is a peripheral 37 kDa palmitoylated phospholipase, and in its absence envelopment is impaired, EEV yield is markedly reduced and the virus is highly attenuated in mice[40,41] (for review, see Smith[39]). The correct intracellular localization of F13L and consequently its proper function depend on the palmitoylation of cysteine residues at positions 185 and 186,[42] and on an intact phospholipase D motif, HKD [motif N-x-K-x(4)-D-x, amino acids 312–327].[43] F13L possesses also a YW motif (positions 253–254), shown to interact with a cellular factor, TIP47, that is associated with late endosome transport vesicle biogenesis. Mutating this motif disrupted F13L–TIP47 interaction.[38] Not only F13L but also the B5R protein is required for the efficient formation of enveloped virions.[40,44] B5R is a transmembrane 42 kDa type I glycoprotein that is palmitoylated and composed of a large extracellular domain and a short cytoplasmic tail.[45] In its absence, wrapping is inhibited, few EEV particles are produced and the virus is attenuated.[46] B5R has been shown to co-localize and interact with F13L[47,48] and, in the presence of ST-246, less immunoprecipitated B5R–F13L complex was found; this might be attributed to (i) mislocalization of F13L and/or B5R or (ii) disruption of the B5R–F13L complex by ST-246.[38]

It remains unclear exactly how ST-246 interferes with F13L. Also, we and others have reported discrepancies in ST-246 antiviral activity between different OPV species, although the compound remains potently active.[21,24,49] Our observations demonstrated that ST-246 differentially inhibited the intra- and extracellular virus production of VACV, CPXV and CMLV in cells and that this may be attributed to dissimilarities in their methods of propagation (which probably involve multiple viral and cellular partners) rather than to differences in F13L sequences.[21,49] In line with this, Santos-Fernandes *et al*.[24] have recently described atypical ST-246 antiviral activity against Cantagalo virus, as this strain appears hypersensitive to the compound, and yet this phenotype was not linked to the presence of the D217N substitution found in the F13L of Cantagalo virus and not in other OPVs. From these observations, one may wonder whether viral proteins other than F13L can play a role in ST-246 efficacy. Here, in addition to identifying the molecular target of ST-246 and investigating how resistance to this drug develops *in vitro* against three OPV species, we provide crucial knowledge with which clinicians may manage patients under ST-246 therapy and identify the potential emergence of drug resistance.

Materials and methods

Viruses, cells and antiviral compounds

The following virus strains were used: CMLV strain Iran (CML1) and strain Dubai (CML14) (provided by the Bundeswehr Institute of Microbiology, Munich, Germany); CPXV strain Brighton (CXPV-BR, ATCC VR-302); VACV strain Copenhagen (VACV-Cop; provided by R. Drillien, CNRS UMR 7104, INSERM U964, Strasbourg, France); VACV strain Western Reserve (VACV-WR, provided by D. Evans, University of Alberta, Edmonton, Canada); and the VACV-WR B5R-deleted version (VACV-WR-ΔB5R, provided by INIA, Madrid, Spain), which has been described elsewhere.[50]

Human embryonic lung fibroblasts (HEL, ATCC CCL-137) and Vero cells (ATCC CCL-81) were grown as previously described.[51] Both cell lines were used for (i) growth of stocks, (ii) selection of drug-resistant viruses and (iii) cell-based assays (for details of media, see Duraffour *et al*.[51]). BSC-1 cells (ATCC CCL-26) were grown in the same medium as that used for Vero cells and used for plaque size assays. Both BSC-1 and HEL cells were used for transfection experiments. BHK21 cells (ATCC CCL-10), used for immunofluorescence experiments, were grown in G-MEM BHK-21 (Gibco, Life Technologies, Belgium) containing 5% FBS, 3 mg/mL tryptose phosphate broth, 0.01 M HEPES, antibiotics and glutamine.

ST-246 [4-trifluoromethyl-N-(3,3a,4,4a,5,5a,6,6a-octahydro-1,3-dioxo-4,6-ethenocycloprop[f] isoindol-2(1H)-yl)-benzamide] was provided by SIGA Technologies Inc. (Corvallis, OR, USA); cidofovir was obtained from Gilead Sciences (Foster City, CA, USA).

Selection of drug-resistant viruses and isolation of clones

CML1, CML14, VACV-Cop and CPXV-BR strains were passaged in HEL cells and/or Vero cells for ∼14–30 passages in the presence of increasing amounts of ST-246, starting at a concentration of 0.001 μg/mL. Depending on the strains and on the cell type, various final doses of ST-246 were used to enable the isolation of drug-resistant viruses (Table 1). Each of these viruses was passaged two or three times in the highest drug concentration and further cultured for two additional passages in drug-free medium. Plaque reduction assays were performed to evaluate the resistant phenotype of the viruses grown under selective pressure with ST-246. Once the resistant phenotype was established by antiviral assays, three to five clones from each of these mutant viruses, as well as from WT strains, were isolated by plaque purification and selected for further genotypic and phenotypic analysis.

Sequencing

Genes were named based on VACV-Cop nomenclature. The following genes were sequenced in each of the WT and ST-246-resistant ($ST\text{-}246^R$) clones: *F13L* (AAA48031), *A27L* (AAA48152), *B5R* (AAA48201), *A33R* (AAA48160) and *A34R* (AAA48161). DNA was extracted from virus-infected cells using the QIAamp® DNA Blood Mini kit (Qiagen Benelux BV, Venlo, The Netherlands) following the manufacturer's instructions. Each gene was amplified as one amplicon using FastStart high-fidelity DNA polymerase (Roche Applied Science, Mannheim, Germany). PCR products were then purified, sequenced and analysed as reported.[51] Data were assembled and compared with DNA sequences obtained for WT viruses using the software SeqScape® version 2.7 (Applied Biosystems Europe BV). Following phenotyping and sequencing, the viruses were named as shown in Table 1.

Table 1. Selection process of ST-246^R viruses and their genotyping

Virus	Cell type	Passages[a]	Final ST-246 concentration (μg/mL)	Gene[b]	Nucleotide change	Amino acid change	Virus identification
VACV-Cop	HEL	17	35	*F13L*	G829T	G277C	VACV-Cop-G277C
	Vero	18	35	*F13L*	T1115A	I372N	VACV-Cop-I372N
CPXV-BR	HEL	19	35	*F13L*	G847T	D283Y	CPXV-BR-D283Y
	Vero	23	100	*F13L*	C580A+Ins908-916CTGTGAAGT	H194N+SVK303–305	CPXV-BR-H194N+SVK303–305
CMLV	HEL	14	20	*F13L*	T73G+T1115A	F25V+I372N	CML1-F25V+I372N
	Vero	14	20	*F13L*	G829T+T1115A	G277C+I372N	CML14-G277C+I372N

[a]Number of passages needed to achieve resistance to ST-246. The last two or three passages were done without drug.
[b]Identification of the gene in which mutation(s) were mapped. Besides *F13L*, the *B5R*, *A27L*, *A33R* and *A34R* genes were sequenced in all drug-resistant and WT clones.

Antiviral assays

ST-246 and cidofovir inhibitory effects against WT and *in vitro*-selected ST-246^R clones were evaluated in HEL cells for the viruses selected on HEL cells, and in Vero cells for the resistant viruses selected on Vero cells. Cells were grown in 96-well microtitre plates. The experimental procedure used has been described previously.[51] Briefly, confluent monolayers were infected at an moi of 0.01 pfu/cell for 2 h, after which residual virus was removed and replaced with medium containing serial dilutions of the test compounds (in duplicate). The viral CPE was recorded after 2–7 days of incubation, depending on the viral strain (i.e. time needed to reach 100% CPE in the control wells). The EC_{50} was calculated as the concentration of a compound required to reduce the viral CPE by 50%. The EC_{50}s of the compounds for each viral strain were calculated as the means of at least three independent determinations.

Virus yields

The antiviral activities of ST-246 and cidofovir were evaluated in HEL and Vero cells infected with WT or ST-246^R clones. Cells were grown in 24-well microtitre plates, and confluent monolayers were infected at an moi of 0.01 pfu/cell. After 2 h of incubation (37°C/5% CO_2), residual virus was removed, each well was washed once with 2 mL of PBS, and serial dilutions of the test compounds were added. After 2–3 days of growth, microtitre plates were frozen at −80°C and thawed, and total virus or cell-associated and extracellular virus was harvested. After centrifugation, virus titres of each sample were determined in the respective cell type (HEL or Vero). Viral titres were expressed in pfu/mL. The 90% and 95% effective concentrations (EC_{90} and EC_{95}) were calculated and defined as the compound concentration required to reduce viral titre by 90% and 95%, respectively.

Viral kinetics

To measure the growth rates of WT and ST-246^R clones, HEL and Vero cells were grown until confluence in 24-well plates and infected with the strain of interest at an moi of 0.01 pfu/cell for 1 h. At the timepoints 3, 6, 8, 24 and 30 h post-infection (hpi), total virus was harvested (in triplicate), and virus was released by freeze–thawing and titrated by plaque assays in HEL or Vero cells. Virus titres, expressed in pfu/mL, are presented as the means of two independent determinations.

Plaque size

BSC-1 cells grown until confluence in six-well microtitre plates were infected with 25–100 pfu per well of the virus of interest, with or without ST-246 (5 μg/mL). After 3 days of incubation, cells were fixed in ethanol and stained with crystal violet, and wells were photographed.

DNA cloning and production of recombinant F13L-mutated viruses

For the production of F13L-mutated recombinant viruses, DNA was extracted from HEL cells infected with the virus of interest, i.e. VACV-Cop-G277C, CML1-F25V+I372N or CML14-G277C+I372N, using QIAamp® DNA Blood Mini (Qiagen Benelux BV). Entire or partial portions of the *F13L* genes were further PCR-amplified with a FastStart high-fidelity DNA polymerase (Roche Applied Science), sequenced and cloned into a pCR®2.1-TOPO® plasmid (Invitrogen, Life Technologies). The cloning reactions were done according to the manufacturer's instructions, and chemically competent DH5α™-T1R was used. The sequence integrity of each plasmid construct was further confirmed by sequencing before proceeding to transfection. The following plasmids were obtained: TOPO-VACV-Cop-G277C, TOPO-CML1-F25V+I372N, TOPO-CML14-G277C and TOPO-CML14-G277C+I372N. Recombinant viruses were produced in HEL cells as they allowed good transfection efficiency. One day prior to infection and transfection, cells were plated at a density of 5×10^5 cells per well in six-well plates. Infection with WT VACV-Cop, CML1 or CML14 occurred at an moi of 1 or 0.5 pfu/cell, for 1 h. Inoculum was removed and cells were replaced in warm medium and returned to the incubator for 2 h. For each construct, the following three transfection conditions were used: 2 μg of plasmid DNA for the moi of 0.5 and 1, and 4 μg of plasmid DNA for the moi of 1 using 10 μL of Lipofectamine™ 2000 (Life Technologies) per well. The plates were incubated for 24 h and the transfection solution was replaced with warm medium. Cells were further cultured for 24 h at 37°C/5% CO_2 and frozen at −80°C. The recombinant viruses were released by freeze–thawing and further grown, at low moi, for two passages in HEL cells in the presence of at least 0.5–1 μg/mL ST-246 in order to eliminate the majority of background WT virus, followed by one last passage without drug. At this stage, one to three stocks of recombinant virus were further used (from one condition or the three separate transfection conditions) and a similar procedure as described[51] was used to isolate and identify recombinant clones. Three isolates originating from each F13L-mutated recombinant parent construct (VACV-Cop-rcb-G277C, CML1-rcb-F25V+I372N, CML14-rcb-G222C and CML14-rcb-G277C+I372N) were obtained after three rounds of plaque purification (in the absence of drug) and retained for further phenotyping.

Production of knock-out F13L viruses

VACV-Cop, CPXV-BR and CML1 viruses deleted in the *F13L* gene (ΔF13L) and expressing an Ecogpt–GFP fusion protein instead were produced by using

synthetic genes (GeneArt®, Life Technologies). They consisted of the sequence of the fusion protein Ecogpt–GFP surrounded by 300 bp of the left and right flanking regions of VACV-Cop, CPXV-BR or CML1 *F13L*. These synthetic genes were present in a pMA-RQ vector (GeneArt®, Life Technologies) and used for further transfection experiments. BSC-1 cells were grown until 80% confluence in six-well plates and infected for 2 h with WT VACV-Cop, CPXV-BR or CML1 at an moi of 1. The inoculum was removed and cells were washed and then transfected with 1 μg of linearized Ecogpt–GFP plasmid per well in medium containing 10 μL of Lipofectamine™ 2000 (Life Technologies). Two days later, samples were frozen at −80°C. Recombinant VACV-Cop-, CPXV-BR- and CML1-ΔF13L clones were further isolated after three to five rounds of plaque purification on Vero cells based on their growth in the presence of an Ecogpt selective medium (containing mycophenolic acid at 0.025 mg/mL, xanthine at 0.25 mg/mL and hypoxanthine at 0.015 mg/mL; see Lorenzo *et al*.[52]) and on GFP expression. Sequence integrity of the recombinant clones was checked by PCR and sequencing. The absence of F13L in the viral genome was further checked by an F13L-specific OPV qPCR.[53]

Production of knock-out B5R viruses

For the production of recombinant VACV-Cop and CML1 deleted in the *B5R* gene (ΔB5R), synthetic VACV-Cop- and CML1-specific DNA fragments were obtained (GeneArt®, Life Technologies). They consisted of the sequence of the fusion protein Ecogpt–GFP (to replace the *B5R* gene) surrounded by 300 bp of the left and right flanking regions of VACV-Cop or CML1 *B5R*. These synthetic genes were present in a vector (pMA-RQ, GeneArt®, Life Technologies) and used for further transfection experiments. The production, isolation and characterization of ΔB5R clones were similar to those of ΔF13L viruses.

Immunofluorescence

BHK-21 cells grown to 70% confluence on round 13 mm coverslips were infected with the different viruses at 5 pfu per cell. One hour after infection, medium was replaced with fresh medium or medium containing 5 μg/mL ST-246. After 18 h, cells were incubated with 2 mg/mL bisbenzimide (Hoechst dye) for 30 min, washed with PBS, fixed for 15 min at room temperature with cold 4% paraformaldehyde in PBS and washed with PBS. Cells were permeabilized by incubation with PBS containing 0.1% Triton X-100 for 15 min. After washing with PBS, cells were incubated for 5 min with PBS containing 0.1 M glycine. Staining was carried out by sequential incubation with primary antibody and secondary antibody, diluted in PBS/20% FBS. Working dilutions were 1:50 for rat anti-F13 MAb, 1:100 for rat anti-B5 and 1:500 for donkey anti-rat IgG–Alexa Fluor 594 (Invitrogen, Life Technologies).

Molecular docking of ST-246 and IMCBH in the binding site of F13L protein

A model of the F13L protein was built using the SWISS-MODEL Workspace[54,55] based on the published structure of *Streptomyces* sp. (strain PMF) phospholipase D (code pdb 1V0W),[56] which shares 77 identical and 115 similar residues with VACV F13L (out of 373 residues). Several modelling portals were investigated to find the most reliable model,[57,58] and the structure of *Streptomyces* phospholipase D was the best hit (code pdb 1V0W; code pdb 2ZE9, unpublished structure; code pdb 1V0S).[56] One other hit, corresponding to the structure of the phosphatidylserine synthase of *Haemophilus influenzae* (code pdb 3HSI) was found, but this structure was unpublished at the time of writing, so we did not proceed with it.[58,59] We still evaluated all four models; their 3D structures appeared similar when superimposed. We ultimately chose a model based on the pdb number 1V0W. ST-246 and IMCBH [*N*(1)-isonicotinoyl-*N*(2)-3-methyl-4-chlorobenzoylhydrazine] were drawn with Molsoft (www.molsoft.com, 2D to 3D converter) and Smiles Translator (http://cactus.nci.nih.gov/services/translate/) to produce the pdb file. Conformation of the structures was checked using the PyMOL graphic system (DeLano Scientific). To perform the docking assays, ArgusLab software (www.arguslab.com) was used. The binding site of ST-246 and IMCBH was delimited using the mutations found in both ST-246- and IMCBH-resistant OPVs and defined using the coordinates of the F13L model. Docking precision was set to 'high' and the 'flexible ligand docking' mode was used for each docking run. Resulting complexes were visualized and pictures were generated with the PyMOL graphic system.

CPXV F13L sequencing and alignments

The *F13L* gene of a total of 65 CPXVs was PCR-amplified and sequenced (GATC, Konstanz. Germany). A total of 99 *F13L* nucleotide sequences available from NCBI (Table 2), 65 CPXV and 2 CMLV in-house sequences were aligned using MEGA 5®, DAMBE® and CLC® workbench software.

Statistical analyses

All statistical analyses were done with GraphPad Prism version 6.00 for Windows (GraphPad Software, La Jolla, CA, USA; www.graphpad.com). The growth rates between WT viruses and recombinant constructs were compared using linear regression analysis as previously described.[51] Briefly, best-fit curves were obtained by transforming the virus titres to their natural logarithm [ln(pfu/mL)], and the derived fit lines were then analysed by linear regression. Statistical significance was only considered for $P \leq 0.05$.

Results

Selection of ST-246^R OPVs and genotyping

ST-246^R viruses were selected in HEL and Vero cells infected with three OPV species: VACV-Cop, CPXV-BR and CMLV (CML1 and CML14). In total, 14–23 passages were needed to select for drug resistance. A detailed overview of the selection process is given in Table 1. Once the drug-resistant phenotype of the viral stocks was confirmed by antiviral assays, two or three clones were used in further experiments. In order to investigate the cause of the drug-resistant phenotype, five viral genes were sequenced based on their roles in intracellular mature virus wrapping (*A27L*, *B5R* and *F13L*) or in the release of enveloped virions from the infected cell (*A33R* and *A34R*) (for review, see Smith *et al*.[60]). As shown in Table 1 and Figure 1, genotyping of each ST-246^R clone revealed that the six mutants harboured mutations in the *F13L* gene, while the *A27L*, *B5R*, *A33R* and *A34R* genes were unaffected. The two VACV-Cop F13L mutants exhibited single amino acid changes, G277C or I372N, the latter corresponding to the last amino acid of the protein. In the two CPXV-BR F13L mutants, the following changes were found: D283Y alone and H194N in combination with an in-frame insertion of nine nucleotides encoding an SVK triplet at positions 303–305. The two F13L-mutant CMLVs bore double amino acid substitutions, F25V+I372N or G277C+I372N; two of these residues had also been identified in the VACV-Cop F13L mutants.

In vitro phenotyping of ST-246^R viruses with mutations in the F13L gene

The impact of the identified mutation(s) on ST-246 and cidofovir antiviral efficacies was evaluated. Cidofovir, one of the reference

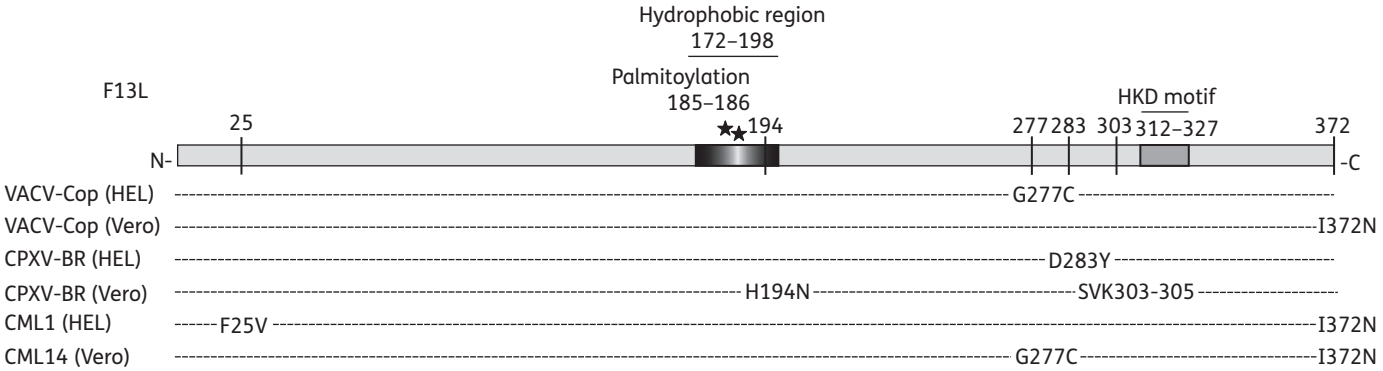

Figure 1. Schematic overview of the amino acid changes identified in F13L of VACV-Cop, CPXV-BR and CMLV strains grown under ST-246 selective pressure. The amino acid changes in each virus are specified with respect to the reference virus for each species. The cell line in which the selection procedure was done is given in brackets.

molecules against poxviruses, acts by blocking the replication of the viral genome and was included as a control. Also, each of the drug-resistant clones was tested in the cell type used for its selection. As shown in Figure 2, levels of resistance to ST-246 varied as a function of the viral strain and of the nature of the mutation(s). ST-246^R VACV-Cop clones showed a 95-fold (G277C, HEL cells) and 9.2-fold (I372N, Vero cells) increase in ST-246 EC_{50} values compared with WT clones. CPXV-BR clones bearing the D283Y change had an ST-246 EC_{50} value increased 44.3-fold [HEL cells, mean EC_{50} 6.2 μM (D283Y) versus 0.14 μM (WT)], whereas in the presence of the double mutation H194N+SVK303–305, the level of resistance in Vero cells was >332.5-fold, with a mean EC_{50} >53.2 versus 0.16 μM (WT). In CMLV, the double mutants F25V+I372N (HEL cells) and G277C+I372N (Vero cells) appeared highly resistant to ST-246, with mean EC_{50} values ≥43 and ≥42 μM, respectively, compared with 0.025 and 0.005 μM for the WT clones. In contrast, all the ST-246^R viruses remained potently inhibited by cidofovir at EC_{50} values in the same range as those of the WT viruses. Of note, the phenotyping of a majority of F13L-mutated viruses selected on HEL cells was also done on Vero cells and *vice versa*, and the levels of ST-246 resistance corroborated the results shown in Figure 2, i.e. mutant viruses showed comparable degrees of ST-246 resistance whether tested on HEL or Vero cells, so that the relative resistance imparted by the mutations can be compared directly (data not shown).

To further confirm the drug-resistant phenotype of the different F13L-mutated clones, virus yield experiments were done. All F13L-mutated strains showed EC_{90} values higher than those of their respective WT virus (Figure S1a, available as Supplementary data at *JAC* Online). While the difference in EC_{90} values between VACV-Cop-VERO-F13L-I372N and its WT counterpart was only 2.7-fold, the calculation of EC_{95} clearly confirmed the drug-resistant phenotype of the I372N strain, with EC_{95}s >53.2 versus 3.56 μM (WT). Importantly, the antiviral efficacy of cidofovir was not altered by the presence of mutation(s) in F13L. These findings corroborated the CPE reduction assays shown in Figure 2. They also confirmed our previously published observations that VACV-Cop, CPXV-BR and CMLV WT viruses exhibit differences in their susceptibility to ST-246, with CPXV-BR being the least susceptible, yet being still potently inhibited at low micromolar concentrations (Figure 2 and Figure S1a).[21,49] Of note, previous work reported that ST-246 was not toxic to proliferating cells, with 50% cytostatic concentrations (CC_{50}s) >532 μM in HEL cells and >40 μM in Vero cells.[19,21] The selectivity indices (ratio of previously reported CC_{50} to EC_{50} obtained in this study) were >3800 (CPXV-BR), >21 280 (CMLV) and >38 000 (VACV-Cop) in HEL cells and >250 (CPXV-BR), >4444 (VACV-Cop) and >8000 (CMLV) in Vero cells.

Growth and plaque size of F13L-mutated viruses

As depicted in Figure S1(b), the growth of F13L-mutant viruses was similar to that of their respective WT counterparts, demonstrating that the presence of the amino acid substitution(s) or insertion did not impact the total virus yield of F13L-mutated viruses in HEL or Vero cells. However, some discrepancies were observed between WT and F13L-mutated strains in terms of average plaque size on BSC-1 cells (Figure 3). The presence of the G277C or the I372N change in VACV-Cop F13L slightly reduced the average size of plaques compared with WT and enveloped viruses appeared to be still released, as evidenced by the comet tail formation. In CPXV-BR, smaller plaques were observed with the D283Y mutant than with the WT virus and the absence of comet tails was indicative of a lack of enveloped virus release. The strain bearing the H194N+SVK303–305 mutations formed slightly smaller comet-shaped plaques than those of the WT virus, but the presence of comet tails suggested that enveloped virus production and release were still occurring. In CML1, the double amino acid change F25V+I372N affected the average size of plaques, which appeared larger than those produced by the WT virus, whereas the G277C+I372N mutations in CML14 did not affect plaque size compared with WT CML14 (Figure 3).

F13L-recombinant viruses confirmed the roles of G277C, G277C+I372N and F25V+I372N in ST-246 resistance

To examine whether the identified mutations were responsible for the drug-resistant phenotype, four recombinant viruses were engineered by introducing the desired *F13L*-mutated gene into a WT virus backbone. This allowed us to study the impact of the G277C change in both VACV-Cop and CML14 backbones, F25V+I372N in CML1 and G277C+I372N in CML14.

The ST-246 EC_{50} value for VACV-Cop-rcb-G277C was 0.29±0.05 μM, whereas it was 0.003±0.0004 μM for VACV-Cop,

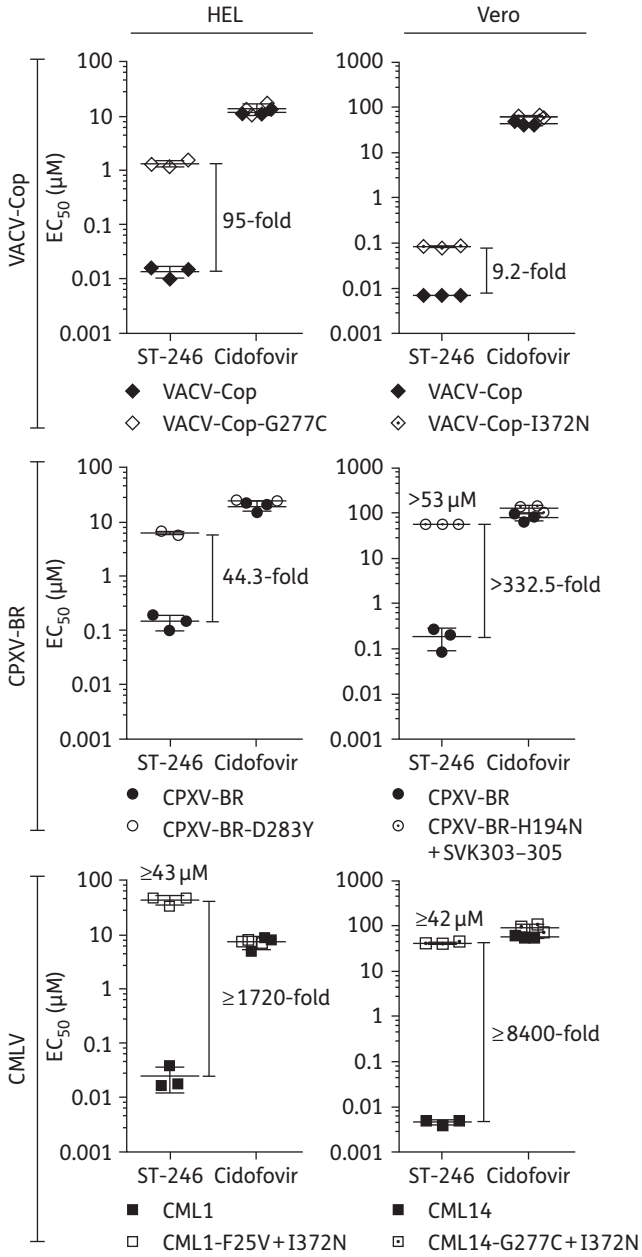

Figure 2. Phenotyping of F13L-mutated VACV-Cop, CPXV-BR and CMLV in HEL and Vero cells. Two or three clones of each WT and ST-246^R clone were used in plaque reduction assays and at least three to five independent experiments were performed per clone and per test compound (ST-246 and cidofovir). Assays were performed in HEL (left-hand panels) and Vero (right-hand panels) cells for the drug-resistant viruses selected in HEL and Vero cells, respectively (refer to Table 1 for names). The data are presented as a dot plot of the EC_{50}s of ST-246^R clones (open symbols) versus the EC_{50}s of WT parent clones (filled symbols). On each graph are shown the fold changes in ST-246 EC_{50} concentrations, which were calculated by dividing the mean of EC_{50}s for ST-246^R clones by the mean of EC_{50}s for WT clones. Results are presented as mean ± SD.

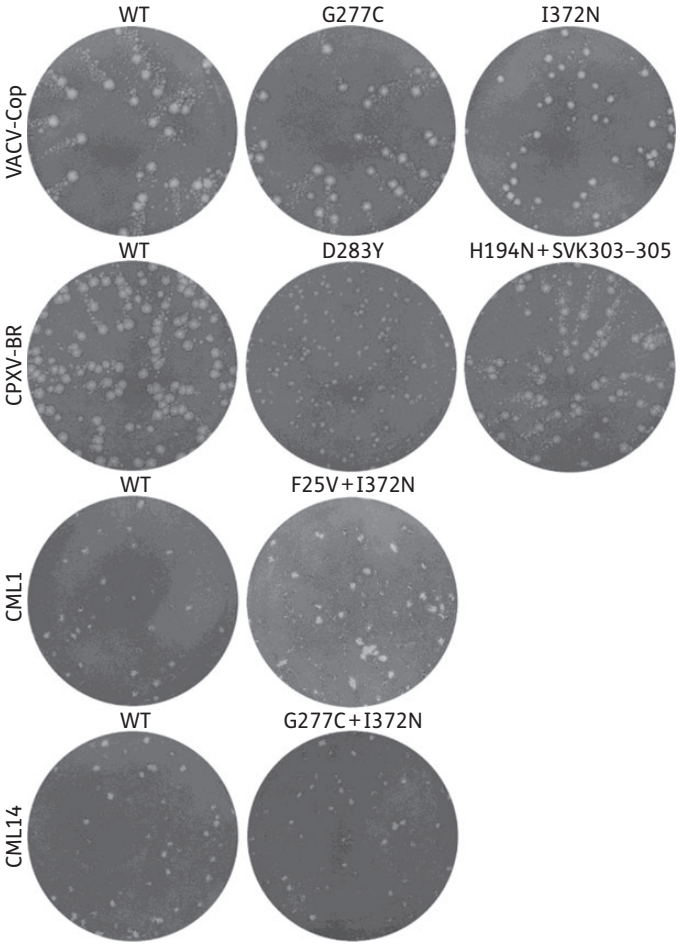

Figure 3. Plaque phenotype under liquid overlay. BSC-1 cells were infected with 25–50 pfu of the indicated strains. At day 3 post-infection, cell monolayers were fixed and stained with crystal violet.

giving 97-fold resistance. This same amino acid change in CML14 led to a 459-fold increase in the ST-246 EC_{50} value (2.29 ± 1.91 versus 0.005 ± 0.03 μM), suggesting that drug resistance levels could be exacerbated in this species compared with VACV-Cop. Adding the I372N change to G277C in CML14 drastically enhanced drug-resistance levels, which were >10639-fold (EC_{50} >53 μM). Recombinant CML1 bearing the F25V+I372N change had reduced susceptibility to ST-246, with an EC_{50} value ≥40 versus 0.007 ± 0.003 μM (WT) (i.e. a ≥5714-fold change in EC_{50}). The drug-resistance levels obtained for the *in vitro*-selected ST-246^R viruses and the recombinant strains were comparable, as shown in Figure S1(c), demonstrating that the amino acid substitutions G277C, G277C+I372N and F25V+I372N are responsible for the ST-246^R phenotype.

Deletion of F13L, but not of B5R, confers ST-246 resistance

To further survey the role of F13L in ST-246 efficacy, knockout F13L and B5R OPVs were engineered. The ΔB5R constructs were included to clarify a possible role of B5R in drug activity as B5R was shown to co-localize and associate with F13L in Golgi cisternae and post-Golgi vesicles.[47,48] Also, mutations in F13L affect the proper localization of B5R in post-Golgi vesicles (e.g. in the absence of F13L, B5R is mainly found in Golgi cisternae).[47] In

turn, B5R mutations have been shown not to influence F13L distribution significantly.[50,61,62]

The two viruses VACV-Cop- and CPXV-BR-ΔF13L were resistant to the drug, with ST-246 EC_{50} values >26.5 μM (Figure 4a). Intra- and extracellular VACV-Cop-ΔF13L production was not altered by the presence of the drug, confirming the drug-resistant phenotype in virus yield assays (Figure 4b). The defect in extra- and intracellular WT virus formation is consistent with our previous observations.[21] Both VACV-Cop- and CPXV-BR-ΔF13L viruses had a small plaque phenotype compared with WT viruses. Interestingly, we have not been able to amplify the CML1-ΔF13L recombinant virus, and this did not allow us to evaluate the effect of ST-246 on this strain. In contrast, the B5R deletion mutants VACV-Cop, VACV-WR and CML1 were potently inhibited by ST-246 at EC_{50}s equivalent to, or even slightly lower than, those of their WT counterparts (Figure 4a). These results present strong evidence that F13L is the target of ST-246.

ST-246 delocalizes both F13L and B5R in infected cells

To get more insight into the antiviral effect of ST-246, we looked at the intracellular localization of F13L and B5R in VACV- and CML1-infected cells, in the absence or presence of ST-246 (Figure 5). The distributions of F13L and B5R have been well characterized in VACV-infected cells.[47,50,62,63] In line with this, following infection with VACV-Cop, VACV-WR or CML1, F13L and B5R accumulated in the Golgi complex area, close to the nucleus, and showed punctate staining in the cytoplasm and in cell projections corresponding to enveloped virus particles. The Golgi complex, as revealed by B5R staining, was more dispersed in CML1-infected cells, compared with VACV-Cop- or VACV-WR-infected cells. Upon ST-246 treatment, F13L and B5R distribution was altered. F13L was delocalized, the Golgi complex was dispersed and diffuse cytosolic staining, with some labelling of the plasma membrane, was noted, as well as the absence of virus particles in projections, suggesting an absence of wrapping. Of note, regions close to the nucleus area of VACV-Cop and -WR remained partially labelled with F13L. Marked cytosolic staining of F13L was seen in CML1-infected treated cells and there was an absence of F13L labelling around the nucleus area. B5R staining also showed disaggregation of the Golgi complex, with B5R localized to fragmented vesicles, although this observation was subtle in CML1. No virus particles in projections were seen. In conclusion, we demonstrated that ST-246 alters the overall distribution of not only F13L, but also B5R. In particular, F13L appears distributed throughout the cytoplasm of the cell when ST-246 is present, which mimics the phenotype seen upon mutation of the HKD phospholipase motif of F13L.[43] These observations also point to a block of virus wrapping by ST-246.

ST-246 does not alter, or only slightly alters, the distribution of F13L in F13L-mutated CPXV-BR

We then explored the effect of F13L mutations on F13L distribution in ST-246^R CPXV-BR and whether ST-246 treatment further impacted F13L localization. Figure 6 shows that F13L localization in CPXV-BR is similar to that in VACV, being mainly localized in the perinuclear area and in enveloped virions. Upon ST-246 treatment F13L was delocalized, giving diffuse cytoplasmic staining in addition to the Golgi labelling. The antiviral effect of ST-246 is also visualized by a decrease in plaque size. The D283Y mutant shows partial delocalization of F13L compared with WT, as demonstrated by increased diffused F13L staining in the cytoplasm. This observation may explain the small plaque size phenotype of the D283Y strain. ST-246 produced only a slight effect, consistent with the intermediate ST-246^R phenotype (44.3-fold

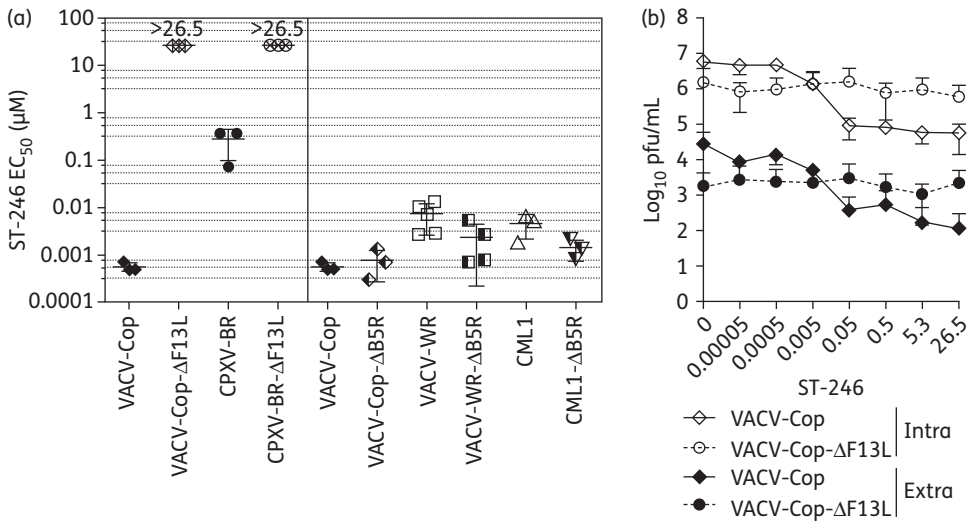

Figure 4. Profiles of the susceptibility of F13L and B5R knockout OPVs to ST-246. (a) Drug-susceptibility profiles of WT, ΔF13L and ΔB5R clones in Vero cells. One clone of each stock was used in CPE reduction assays with ST-246, and at least three independent experiments were performed. The results are presented as a dot plot of the EC_{50}s (mean ± SD). EC_{50}s >26.5 μM were obtained with the two ΔF13L viruses. The fold change in ST-246 EC_{50} values was calculated as the ratio of mean EC_{50} for ΔF13L to mean EC_{50} for WT; it was >44 167-fold for VACV-Cop-ΔF13L (EC_{50} >26.5 μM) versus VACV-Cop (EC_{50} = 0.0006 ± 0.00007 μM) and >98-fold for CPXV-BR-ΔF13L (EC_{50} >26.5 μM) versus CPXV-BR (EC_{50} = 0.27 ± 0.17 μM). (b) Virus yields. Confluent Vero cells were infected with the indicated virus at an moi of 0.01 pfu per cell for 2 h, after which serial concentrations of ST-246 (μM) were added for 2 days. Extracellular (supernatant) and intracellular (cell-associated) fractions were collected and virus titres determined. Three independent experiments were performed and the data are presented as mean ± SD.

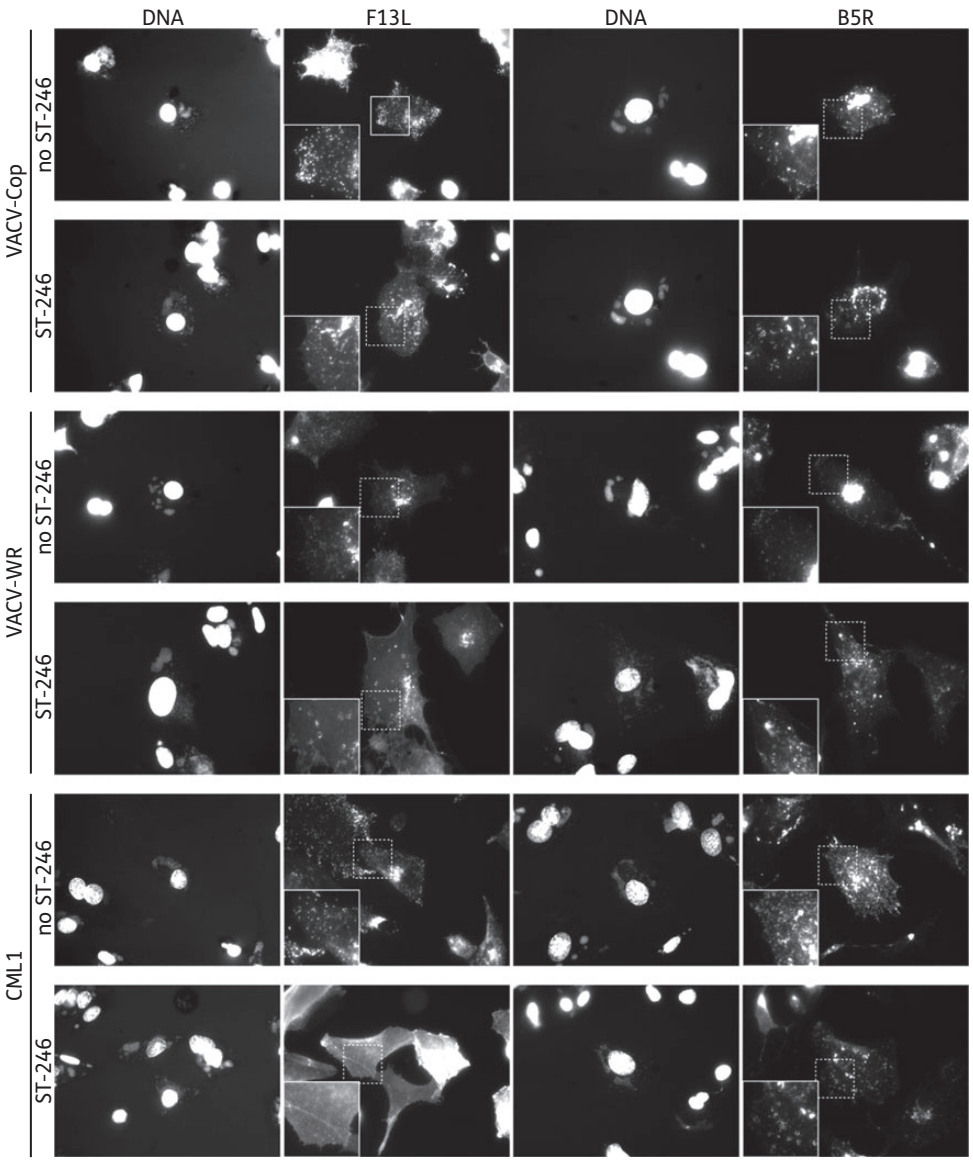

Figure 5. Intracellular localization of F13L and B5R in cells infected with WT viruses in the absence or presence of ST-246. BHK-21 cells infected with VACV-Cop, VACV-WR or CML1 for 18 h at an moi of 5 pfu per cell in the absence or presence of ST-246 (5 μg/mL) were subjected to immunofluorescence analysis. DNA was stained by incubation with Hoechst dye for 30 min at the end of the infection period. F13L was stained with rat anti-F13 antibody and B5R with rat anti-B5R antibody, both followed by donkey anti-rat Alexa Fluor 594 antibody. Note the delocalization of F13L and B5R upon treatment with ST-246, as evidenced by Golgi complexes appearing in fragmented vesicles, a diffuse cytoplasmic staining of F13L (especially marked with VACV-WR and CML1) and the absence of the spotted staining normally corresponding to virus particles in cells and cell projections. Inserts show zoom-ins of squared regions.

shift in EC_{50}; Figure 2) and the reduced average plaque size (Figure 6). Similar observations were made with the mutant bearing the H194N + SVK303–305 changes in terms of F13L staining. Yet this mutant had less delocalized F13L than the D283Y mutant and F13L distribution was not significantly changed by ST-246 treatment, which is in line with the level of resistance (>332.5-fold; Figure 2), the average plaque size and the production of comet tails. Together, these data proved that, despite the slight F13L cytoplasmic staining due to the presence of the D283Y or H194N + SVK303–305 change(s), adding ST-246 did not further significantly delocalize or only slightly (D283Y) delocalized F13L, in agreement with their resistant phenotypes.

Putative model and molecular docking of F13L/ST-246

The molecular characterization of ST-246^R viruses enabled the mapping of F13L residues that are implicated in ST-246 antiviral efficacy, including F25, H194, G277, D283, SVK303–305 and I372. Also, IMCBH inhibits OPVs by targeting the F13L protein,[44] and selection of IMCBH-resistant (IMCBH^R) VACV led to the identification of single amino acid substitutions in F13L responsible for drug resistance, including H238Q, N267D, D283G, A288P and D294V. Interestingly, some of these IMCBH^R mutants were also resistant, or partially resistant, to ST-246. In particular, the mutant bearing the A288P change rendered the virus effectively

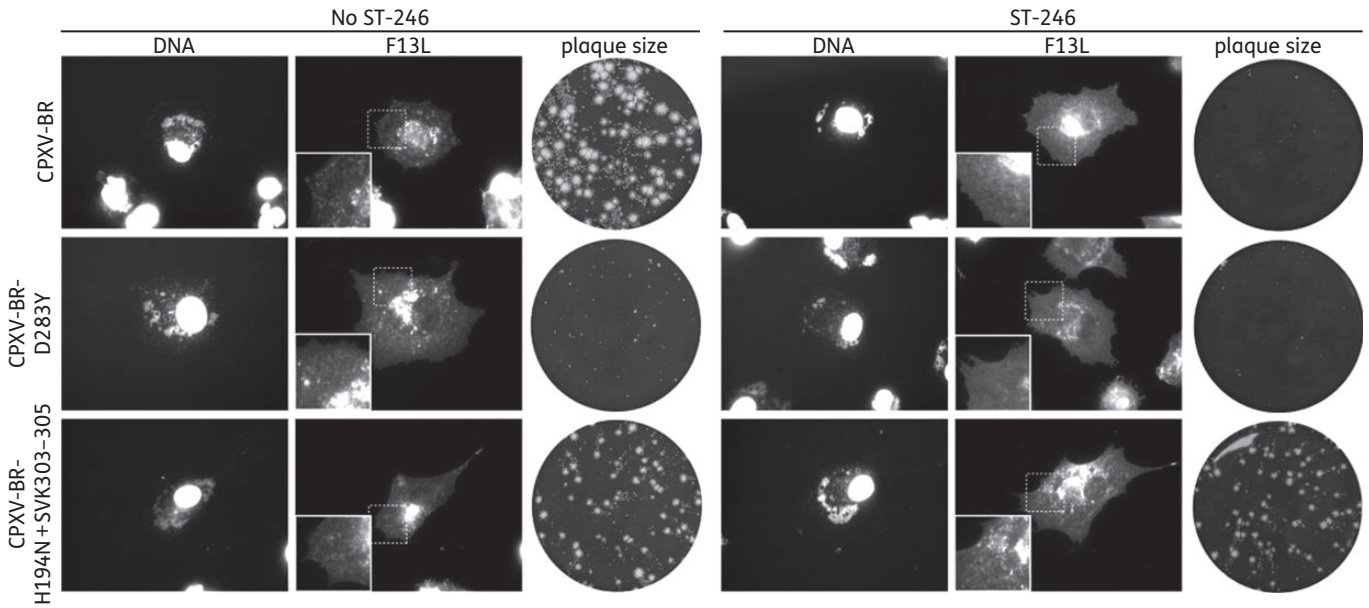

Figure 6. Intracellular distribution of F13L and plaque size in cells infected with WT or F13L-mutated CPXV-BR viruses in the absence or presence of ST-246. BSC-1 (plaque size) or BHK-21 (immunofluorescence) cells were infected with the indicated virus for, respectively, 3 days (moi 100 pfu per cell) or 18 h (moi 5 pfu per cell) in the absence or presence of ST-246 (5 μg/mL). To determine plaque size, cell monolayers were fixed in ethanol and stained with crystal violet and photographs were taken. To assess immunofluorescence, DNA was stained by incubation with Hoechst dye for 30 min at the end of the infection period. F13L was stained with rat anti-F13 antibody followed by donkey anti-rat Alexa Fluor 594 antibody. Inserts show zoom-ins of squared regions.

resistant to both drugs, reflecting the importance of the A288 residue for ST-246 inhibitory effect (R. Blasco, unpublished results). All these findings were compiled and integrated into a putative model of VACV F13L.

Since a 3D structure of VACV F13L does not exist, we built a putative model based on the published structure of *Streptomyces* sp. phospholipase D,[56] which was found to be the most reliable structure to model the F13L phospholipase (Figure 7a). It was then used for further molecular docking of F13L and ST-246 or IMCBH (Figure 7b–d).

The majority of the residues involved in ST-246 resistance development were localized close to each other, with the exception of F25 and H194. They delimited an area within a pocket in which not only ST-246 but also IMCBH were predicted to interact, and both inhibitors were superimposed in this pocket (Figure 7b). The interaction site of ST-246/F13L was formed in particular by the residues G277, W279, D280, A288, A289, A290, L302, S303, V304, K305, V306 and F307 (Figure 7c). The three fluorine atoms of ST-246 (spaced by 2.4 Å) penetrated this relatively small pocket, as evidenced by the distances between the lateral chains of A288–A290 (4.71 Å), A290–V304 (5.28 Å) and V304–W279 (5.83 Å), whereas the benzamide moiety fitted at the interface formed by W279 and V304. At the opposite side of the interaction site was found the H(N)KD phospholipase motif (Figure 7d).

ST-246^R mutations were not found in F13L OPV sequences

F13L amino acid alignments were performed to check whether the amino acid substitution(s) or insertions identified in this study were found as natural polymorphisms. This was done with sequences available in NCBI, but recent phylogenetic data led us to include additional CPXV strains in this analysis since CPXVs have been shown to have relatively high genomic heterogeneity.[64] As shown in Table 2, a total of 166 F13L OPV nucleotide sequences were collected (99 from NCBI, 2 in-house CMLVs and 65 newly sequenced CPXVs), and from these 70 unique F13L gene sequences were identified. Of note, no nucleotide duplicates were found across virus species. CPXV and VACV showed marked heterogeneity, as evidenced by a count of, respectively, 36 and 16 unique gene sequences that originated from 77 and 22 *F13L*, which contrasted with that of other OPVs (e.g. 8 unique sequences derived from 49 nucleotide sequences in VARVs). These 70 unique genes were translated into 41 unique F13L amino acid sequences. While most of them were OPV specific, identical F13L sequences were found between CPXV/VARV and CPXV/VACV (Table 3). Protein alignments further revealed that no naturally occurring ST-246^R viruses were found. In fact, the entire regions where amino acid substitution(s) or insertions linked with the drug-resistant phenotype were identified, appeared highly conserved between the strains (Figure S2).

Discussion

Here we present for the first time an extensive report about the identification of the molecular target of ST-246 in three OPV species, VACV, CPXV and CMLV. Previous work published by our group and others had shown (i) that one point mutation (G277C) in F13L was responsible for ST-246 resistance and (ii) that the drug inhibited the production and/or release of enveloped virions from the cell (e.g. using electron microscopic examination and small interfering RNAs).[19,21,49] Yet it remained crucial to investigate the

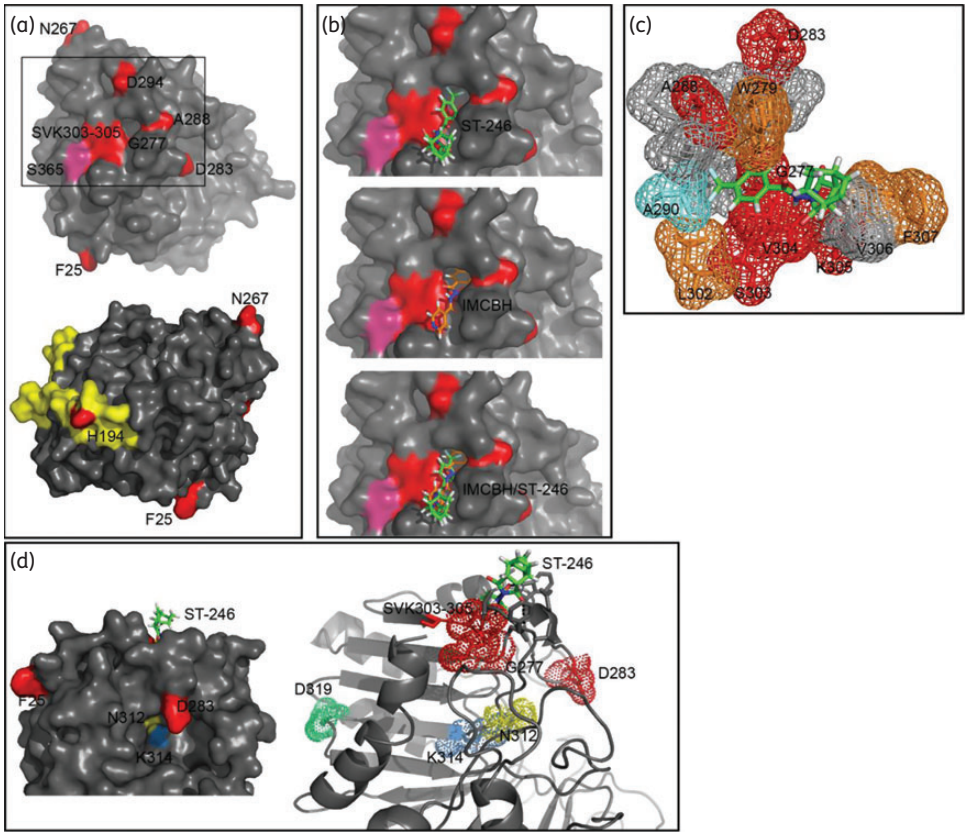

Figure 7. F13L modelling and molecular docking of F13L/ST-246. The structure of *Streptomyces* sp. (strain PMF) phospholipase D (code pdb 1V0W) was used to build a putative model of the F13L protein.[56] (a) Overview of the F13L putative 3D structure highlighting the residues important for ST-246 and/or IMCBH antiviral efficacy. The insert corresponds to the region defined for molecular docking. The putative hydrophobic region (172–198) that anchors F13L in cellular membranes is shown in yellow. (b) Docking of F13L with ST-246 or IMCBH revealing the presence of a pocket in which both of the molecules fit. (c) Close-up view of interaction site between F13L and ST-246 formed by G277, W279, D280, A288, A289, A290, L302, S303, V304, K305, V306 and F307. Note that the three fluorine atoms penetrate the pocket, while the benzamide moiety locates at the interface formed by W279 and V304. (d) Surface view (left-hand panel) and close-up view (right-hand panel) of the H(N)KD motif located opposite to the ST-246 interaction site. Binding of ST-246 may directly interfere with the flexibility of the chain bearing N312 and K314, which form the phospholipase motif. Red, residues found to be linked with ST-246 resistance and IMCBH resistance; cyan (A290), the change A290V was identified in a patient that received ST-246 therapy;[37] orange and grey in (c), additional residues forming the interaction site of the inhibitor; yellow (N312), blue (K314) and green (D319), residues corresponding to the H(N)KD phospholipase motif; magenta (S365), residue corresponding to the last amino acid (S365) that could be integrated in the modelling. The last 7 amino acids of F13L (372 amino acids) could not be included in the modelling.

following questions. How does ST-246 interfere with its probable target? Are there other viral proteins involved in its activity? What about the barrier to resistance? Can we provide a list of well-characterized mutations to facilitate drug-resistance surveillance? To answer these questions, we chose complementary approaches consisting of: (i) selecting drug-resistant variants to identify the viral genetic modifications causing drug resistance; (ii) using knock-out mutants to confirm the target's identity; (iii) building a 3D model coupled with molecular docking to visualize drug–target interaction; and (iv) performing F13L sequence comparisons among OPVs to ensure the absence of drug-resistance loci. Together, our results demonstrate that F13L is a direct target of ST-246 and strongly suggest that the drug delocalizes F13L and either directly or indirectly disrupts the biological function of the protein.

During the isolation of ST-246^{R} mutants, two independent selection processes in each virus species (i.e. on HEL and Vero cells) led to the mapping of amino acid changes in F13L, and not in other proteins needed for the envelopment of virions or the release of EEV from the cell (i.e. B5R, A27L, A33R and A34R). While we did not perform whole-genome sequencing, the various F13L- and B5R-recombinant strains produced for this study strongly point to the absence of mutations in genes other than *F13L*. We clearly demonstrated that the mutations (e.g. G277C, G277C+I372N, F25V+I372N) are responsible for the drug-resistant phenotype and that ST-246 lacked activity in the absence of F13L. This was not seen with the ΔB5R viruses, against which ST-246 conserved its antiviral efficacy. We further noted that the deletion of F13L, as compared with the WT virus, decreased extracellular VACV-Cop titres at 48 hpi by ∼1.25 $\log_{10}$ in the absence of ST-246 (Figure 4b), which is in line with the role of F13L in EEV production impairment.[40,41] Similarly, 0.5 μM ST-246 (compared with no drug) reduced extracellular VACV-Cop WT production by ∼1.6 $\log_{10}$ (Figure 4b), suggesting comparable effects between deleting F13L and inhibiting the function of F13L with ST-246.

The number of passages required to isolate drug-resistant variants varied from 14 to 23 (requiring 6 months to 1.5 years) and the final concentrations of ST-246 used were at least 10000-fold higher than the EC_{50}s. This demonstrates that there was a relatively high barrier to resistance. In line with this, we were unable to isolate one drug-resistant variant of CML14 that was grown in HEL cells for >40 passages (~2 years) under ST-246 pressure. Of note, Yang *et al.*[19] isolated a CPXV mutant with the G277C change after one round of selection using a high infectious dose (10^7 pfu per well) and an ST-246 dose of 10 μM. The progressive exposure to ST-246 and the low moi used in our selection processes may explain these differences.

Table 2. F13L nucleotide heterogeneity among different OPV species

OPV species	Total number of F13L nucleotide sequences	Number of unique F13L nucleotide sequences
VARV	49	8
MPXV	10	5
VACV	22	16
CPXV	77[a]	36
CMLV	4[b]	2
ECTV	3	2
TATV	1	1
Total	166	70

MPXV, monkeypox virus; ECTV, ectromelia virus; TATV, taterapox virus.
A total of 166 F13L OPV sequences were obtained from NCBI or by in-house sequencing. Using MEGA 5® and DAMBE®, 70 unique nucleotide sequences were identified.
See Table 3 and Figure S2 for the count of unique amino acid sequences and protein alignments performed using the 41 unique amino acid sequences derived from the 70 unique nucleotide sequences.
[a]Including 12 NCBI CPXV sequences and 65 in-house CPXVs.
[b]Including two NCBI CMLV sequences and two in-house CMLVs (CML1 and CML14).

Nevertheless, these results demonstrate that the G277C change is critical for ST-246 efficacy in three different OPV species.

One may wonder whether the concentrations of ST-246 used for drug-resistance selection may relate to blood exposures in humans. While the appearance of drug resistance in patients is of high concern and priority, it appears difficult to answer this question as our work was done in cell monolayers, after multiple passages in increasing concentrations of ST-246 and over a quite long period of time, which may not reflect patient's exposure to ST-246 therapy. Also, several animal studies have been done with ST-246 and resistance has never been reported. However, one case report describes an ST-246^R VACV (A290V and L315M in F13L identified by pyrosequencing) in an immunosuppressed patient with progressive vaccinia and receiving multiple treatments including ST-246 (given for 73 days orally and 68 days topically), VIGIV (vaccinia immune globulin intravenous) and CMX001 (oral derivative of cidofovir).[37] The ST-246 EC_{50} values for the virus collected from the vaccination site lesion were increased by 13.5- to 50-fold, and the infection eventually resolved. In immunocompetent individuals, the mode of action of ST-246 is to hold the virus in check until the immune system is activated and clears the virus. Thus, in immunocompromised patients a longer treatment period may be needed and may eventually lead to the appearance of resistance. To diminish the potential risk of emergence of viruses with altered drug susceptibility, combination therapy consisting of ST-246 and molecules aimed at viral DNA replication inhibition (cidofovir, CMX001) should definitely be considered[23,65] and may best be initiated at disease onset.[37] ST-246 and CMX001 combination treatment has been shown to be synergistic *in vitro* and *in vivo*.[23] We also showed here that cidofovir has antiviral potency against all ST-246^R viruses *in vitro*.

In our hands, the levels of ST-246 resistance were directly correlated to the virus species and the nature of the mutation. For instance, the G277C change led to changes in EC_{50} values of 95-fold in VACV, 459-fold in CMLV and 800-fold in CPXV.[19] Such discrepancies could be related to differences in F13L requirement for virus wrapping, which is in line with our previous hypothesis.[21,49] In VACV, virus wrapping is very dependent on F13L, but cell-to-cell transmission of viruses completely relies on virus envelopment.[40,66]

Table 3. F13L amino acid heterogeneity between OPV species

Virus species	VARV	MPXV	VACV	CPXV	CMLV	ECTV	TATV	Total per virus	Total all species
VARV	6	—	—	1	—	—	—	7	
MPXV		3	—	—	—	—	—	3	
VACV			9	1	—	—	—	10	
CPXV				17	—	—	—	17	41
CMLV					2	—	—	2	
ECTV						1	—	1	
TATV							1	1	
Total per virus	6	3	9	19	2	1	1		
Total all species				41					

MPXV, monkeypox virus; ECTV, ectromelia virus; TATV, taterapox virus.
Cross-tabulation of F13L amino acid sequences obtained from the 70 unique F13L nucleotide sequences, numbered per virus species (Total per virus) or among all OPVs (Total all species).

While in VACV and CPXV there may be a small contribution of proteins other than F13L to give basal virus envelopment activity, our results led us to speculate that this might not be the case for CMLV. Indeed: (i) we were unable to obtain a stock of CML1-ΔF13L; (ii) the few infected cells did not form the typical syncytia of CMLV (as seen in Vero and BSC-1 cells); (iii) CMLV was very susceptible to ST-246; and (iv) the levels of resistance were exacerbated in this virus backbone. It could be that these features relate to sequence diversity of CMLV F13L or that CMLV depends exclusively on F13L for virus wrapping. Considering the latter suggestion, it may be that CMLV F13L evolved to act more independently of other viral proteins, so that, because all virus envelopment relies on F13L, susceptibility to ST-246 may be higher. Thus, delocalization of F13L in CMLV may also be higher under drug treatment, and this matches our observations. We also observed an atypical B5R localization pattern with CMLV compared with VACV, which reinforces the idea that CMLV might have a peculiar wrapping process. It remains to be explored whether this phenotype relies on F13L alone or whether F13L deletion/mislocalization disrupted interaction with other viral/cellular proteins necessary for CMLV wrapping and transmission.

F13L-mutated viruses replicated similarly to and had fitness (i.e. total virus yields) comparable to that of WT viruses. Nevertheless, the small plaques produced by the CPXV-BR-D283Y strain may be correlated to the partial delocalization of the F13L protein due to the presence of the D283Y change, as observed in immunofluorescence analysis. The same may be true for H194N + SVK303–305 and can be hypothesized for the G277C substitution found in VACV-Cop. One may ask whether mutations elsewhere in the genome could be responsible for the small plaque phenotype of the D283Y strain, as its recombinant counterpart was not engineered, but the fact that VACV-Cop-rcb-G277C shared the same features (e.g. resistance level and plaque size) as the *in vitro*-selected VACV-Cop-G277C let us speculate that this is not the case. Future work should still aim to investigate whether such viruses are equally virulent as WT strains in animal hosts. Indeed, fitness *in vitro* does not necessarily translate to fitness or virulence *in vivo*.

Together, our data enable us to hypothesize about the mode of action of ST-246. We observed that F13L was still present in the cell upon ST-246 treatment but the protein was delocalized, as evidenced by diffuse cytoplasmic staining, the Golgi complex being dispersed and the fact that no virus was seen in projections. ST-246 does not seem to interfere with F13L production[49] but instead prevents its normal localization in the cell. Nevertheless, F13L may still be found in regions close to the nucleus in large vesicles (Figure 5; VACV-Cop and -WR). This may explain why Chen *et al*.[38] observed co-localization of F13L with *trans*-Golgi network markers in the presence of ST-246. ST-246, and also IMCBH, were predicted to fit in a pocket formed from amino acids that are highly conserved among all OPV F13L proteins, which is oriented in opposition to the phospholipase H(N)KD motif (Figure 7). Roper and Moss[43] demonstrated that mutating the HKD motif led to wrapping impairment, a failure of F13L to concentrate in the Golgi area and F13L was distributed throughout the cell, partly mimicking our findings, i.e. F13L may still be found in the Golgi area, as seen with VACV and CPXV. Indeed, F13L exhibits broad-specificity lipase activities *in vitro*, possessing triacylglycerol lipase and phospholipase A and C activities,[67] which directly or indirectly contributes to the formation of the virus-modified wrapping cisternae or post-Golgi vesicles that will further envelope virions.[63] One interpretation could be that, when interacting, ST-246 may directly disturb the loop bearing the residues N312 and K314 of the H(N)KD motif and thus interfere with the conformation of the phospholipase motif. This would then partially prevent the proper localization and/or trafficking of the F13L protein and, as a consequence, impair the envelopment and release of extracellular viruses. Other possibilities could be that the pocket in which ST-246 fits, or its close surroundings, has a yet-unknown function needed for F13L intracellular trafficking, targeting into the Golgi and/or production of enveloped viruses. The report of A290V and/or L315M changes isolated from a patient under ST-246 therapy may favour the first hypothesis.[37] The A290 amino acid forms the pocket in which the three fluorine atoms of ST-246 (spaced by 2.4 Å) enter, and the L315 residue is immediately next to K314, which forms the H(N)KD motif (Figure 7). The cross-resistance between ST-246 and IMCBH when the change A288P is present reinforces our working model.

However, the last amino acids of VACV F13L could not be modelled, so that it was not possible to evaluate the impact of the I372N change, but the last amino acid modelled (S365) was localized close to the binding pocket. Also, the H194N substitution mapped to the hydrophobic region and this may explain the slight delocalization of the F13L seen in this mutant. The SVK303–305 insertion duplicates the pre-existing SVK triplet, along which the benzamide moiety of ST-246 is found. This may explain why ST-246 no longer binds within the pocket when the insertion is present (according to *in silico* modelling). The N-terminal amino acid change F25V appears quite distant from the binding site and the HKD motif, making it difficult to assess its potential role in drug resistance. This change could stabilize the I372N substitution, but further studies should assess its impact on ST-246 resistance. Our 3D model coupled to molecular docking remains hypothetical, but is currently the only existing model available to estimate the probable folding of VACV F13L. Only the *in vitro* expression of F13L and the resolution of its 3D structure will help in reaching more certain conclusions.

Finally, we showed that none of the amino acid changes identified in this study and described in the literature[19,37] was related to polymorphisms among 166 OPV F13L sequences. The 65 newly sequenced CPXV *F13L* genes confirmed the genomic heterogeneity found among this virus species with 36 unique nucleotide sequences. However, their translation into amino acid sequences highlighted that one sequence was identical between CPXV and VACV and another was identical between CPXV and VARV. These alignments demonstrated also that the regions targeted by ST-246 (based on resistance analysis) were highly conserved between the species, as were the residues forming the ST-246-binding pocket and the phospholipase motif. The residue at position 291 showed some variability among OPVs (R, K or E) and is located deep in the pocket accommodating the three fluorine atoms, and it may be that it slightly alters the efficacy of ST-246 (R291 in VACV-Cop versus K291 in CPXV-BR).

In conclusion, we confirmed that ST-246 is a broad-spectrum antiviral among OPVs and showed that acquisition of ST-246 resistance was a long process *in vitro* when using our method of selection. F13L was identified as a direct target of the drug and a detailed characterization of the various mutants provides for the first time a tool to efficiently monitor the appearance of drug resistance. We showed that ST-246 prevents the normal localization of F13L in three different OPV species. We also provide the first

putative modelling of the F13L/ST-246 interaction site, which is delimited by the majority of the amino acids demonstrated to alter ST-246 antiviral activity when mutated. Together, our data show that ST-246 acts as a key to lock F13L. This research also paves the way to further study of the wrapping process between OPVs, in particular that of CMLV. Beyond OPVs, our work emphasizes the benefit of a molecule targeting virus wrapping. Such an approach should be considered for other enveloped viruses as these molecules may exhibit properties similar to ST-246, including marked specificity, potent activity and a high barrier to resistance.

Acknowledgements

We are thankful for the excellent technical assistance provided by Steven Carmans, Lies Van den Heurck, Anita Camps and Pierre Fiten, the technical advice given by Robert Drillien regarding the engineering of deleted recombinant viruses, the help of Annabel Rector in processing F13L nucleotide sequences and the support given by Robert Jordan when this project was initiated.

Funding

This work was funded by the Belgian grants Fonds Wetenschappelijk Onderzoek (grant number FWO G-0608-08), Geconcerteerde Onderzoeksacties (grant number GOA 10/014) and Program Financing (PF/10/018), and grant RTA2013-00021-00-00 from the Spanish Programa estatal de I+D+I orientada a los retos de la sociedad.

Transparency declarations

D. G. and D. E. H. are employees of SIGA Technologies Inc. All other authors: none to declare.

Supplementary data

Figures S1 and S2 are available as Supplementary data at *JAC* Online (http://jac.oxfordjournals.org/).

References

1 Shchelkunov SN. An increasing danger of zoonotic orthopoxvirus infections. *PLoS Pathog* 2013; **9**: e1003756.

2 Favier AL, Flusin O, Lepreux S *et al*. Necrotic ulcerated lesion in a young boy caused by cowpox virus infection. *Case Rep Dermatol* 2011; **3**: 186–94.

3 Haase O, Moser A, Rose C *et al*. Generalized cowpox infection in a patient with Darier disease. *Br J Dermatol* 2011; **164**: 1116–8.

4 Pelkonen PM, Tarvainen K, Hynninen A *et al*. Cowpox with severe generalized eruption, Finland. *Emerg Infect Dis* 2003; **9**: 1458–61.

5 Vogel S, Sardy M, Glos K *et al*. The Munich outbreak of cutaneous cowpox infection: transmission by infected pet rats. *Acta Derm Venereol* 2012; **92**: 126–31.

6 Schatzmayr HG, Costa RV, Goncalves MC *et al*. Human and animal infections by vaccinia-like viruses in the state of Rio de Janeiro: a novel expanding zoonosis. *Vaccine* 2011; **29** Suppl 4: D65–9.

7 Medaglia ML, Pessoa LC, Sales ER *et al*. Spread of Cantagalo virus to northern Brazil. *Emerg Infect Dis* 2009; **15**: 1142–3.

8 Bhanuprakash V, Venkatesan G, Balamurugan V *et al*. Zoonotic infections of buffalopox in India. *Zoonoses Public Health* 2010; **57**: e149–55.

9 McCollum AM, Damon IK. Human monkeypox. *Clin Infect Dis* 2014; **58**: 260–7.

10 Duraffour S, Meyer H, Andrei G *et al*. Camelpox virus. *Antiviral Res* 2011; **92**: 167–86.

11 McCollum AM, Austin C, Nawrocki J *et al*. Investigation of the first laboratory-acquired human cowpox virus infection in the United States. *J Infect Dis* 2012; **206**: 63–8.

12 Riyesh T, Karuppusamy S, Bera BC *et al*. Laboratory-acquired buffalopox virus infection, India. *Emerg Infect Dis* 2014; **20**: 324–6.

13 Laboratory-acquired vaccinia virus infection—Virginia, 2008. *MMWR Morb Mortal Wkly Rep* 2009; **58**: 797–800.

14 Laboratory-acquired vaccinia exposures and infections—United States, 2005–2007. *MMWR Morb Mortal Wkly Rep* 2008; **57**: 401–4.

15 Kaiser J. *Six Vials of Smallpox Discovered in U.S. Lab*. 2014. http://news.sciencemag.org/health/2014/07/six-vials-smallpox-discovered-u-s-lab.

16 Green A. Ebola emergency meeting establishes new control centre. *Lancet* 2014; **384**: 118.

17 Cleton N, Koopmans M, Reimerink J *et al*. Come fly with me: review of clinically important arboviruses for global travelers. *J Clin Virol* 2012; **55**: 191–203.

18 Enserink M. Mission to MERS. *Science* 2014; **344**: 1218–20.

19 Yang G, Pevear DC, Davies MH *et al*. An orally bioavailable antipoxvirus compound (ST-246) inhibits extracellular virus formation and protects mice from lethal orthopoxvirus challenge. *J Virol* 2005; **79**: 13139–49.

20 Berhanu A, King DS, Mosier S *et al*. ST-246 inhibits in vivo poxvirus dissemination, virus shedding, and systemic disease manifestation. *Antimicrob Agents Chemother* 2009; **53**: 4999–5009.

21 Duraffour S, Snoeck R, de VR *et al*. Activity of the anti-orthopoxvirus compound ST-246 against vaccinia, cowpox and camelpox viruses in cell monolayers and organotypic raft cultures. *Antivir Ther* 2007; **12**: 1205–16.

22 Huggins J, Goff A, Hensley L *et al*. Nonhuman primates are protected from smallpox virus or monkeypox virus challenges by the antiviral drug ST-246. *Antimicrob Agents Chemother* 2009; **53**: 2620–5.

23 Quenelle DC, Prichard MN, Keith KA *et al*. Synergistic efficacy of the combination of ST-246 with CMX001 against orthopoxviruses. *Antimicrob Agents Chemother* 2007; **51**: 4118–24.

24 Santos-Fernandes E, Beltrame CO, Byrd CM *et al*. Increased susceptibility of Cantagalo virus to the antiviral effect of ST-246®. *Antiviral Res* 2012; **97**: 301–11.

25 Sbrana E, Jordan R, Hruby DE *et al*. Efficacy of the antipoxvirus compound ST-246 for treatment of severe orthopoxvirus infection. *Am J Trop Med Hyg* 2007; **76**: 768–73.

26 Smith SK, Olson VA, Karem KL *et al*. In vitro efficacy of ST246 against smallpox and monkeypox. *Antimicrob Agents Chemother* 2009; **53**: 1007–12.

27 Smith SK, Self J, Weiss S *et al*. Effective antiviral treatment of systemic orthopoxvirus disease: ST-246 treatment of prairie dogs infected with monkeypox virus. *J Virol* 2011; **85**: 9176–87.

28 Jordan R, Goff A, Frimm A *et al*. ST-246 antiviral efficacy in a nonhuman primate monkeypox model: determination of the minimal effective dose and human dose justification. *Antimicrob Agents Chemother* 2009; **53**: 1817–22.

29 Nalca A, Hatkin JM, Garza NL *et al*. Evaluation of orally delivered ST-246 as postexposure prophylactic and antiviral therapeutic in an aerosolized rabbitpox rabbit model. *Antiviral Res* 2008; **79**: 121–7.

30 Quenelle DC, Buller RM, Parker S *et al*. Efficacy of delayed treatment with ST-246 given orally against systemic orthopoxvirus infections in mice. *Antimicrob Agents Chemother* 2007; **51**: 689–95.

31 Chinsangaram J, Honeychurch KM, Tyavanagimatt SR *et al*. Safety and pharmacokinetics of the anti-orthopoxvirus compound ST-246 following a single daily oral dose for 14 days in human volunteers. *Antimicrob Agents Chemother* 2012; **56**: 4900–5.

32 Jordan R, Chinsangaram J, Bolken TC *et al*. Safety and pharmacokinetics of the antiorthopoxvirus compound ST-246 following repeat oral dosing in healthy adult subjects. *Antimicrob Agents Chemother* 2010; **54**: 2560–6.

33 Leeds JM, Fenneteau F, Gosselin NH *et al*. Pharmacokinetic and pharmacodynamic modeling to determine the human dose of ST-246® to protect against smallpox. *Antimicrob Agents Chemother* 2012; **57**: 1136–43.

34 Chinsangaram J, Honeychurch KM, Tyavanagimatt SR *et al*. Pharmacokinetic comparison of a single oral dose of polymorph form I versus form V capsules of the antiorthopoxvirus compound ST-246 in human volunteers. *Antimicrob Agents Chemother* 2012; **56**: 3582–6.

35 Berhanu A, King DS, Mosier S *et al*. Impact of ST-246® on ACAM2000 smallpox vaccine reactogenicity, immunogenicity, and protective efficacy in immunodeficient mice. *Vaccine* 2010; **29**: 289–303.

36 Vora S, Damon I, Fulginiti V *et al*. Severe eczema vaccinatum in a household contact of a smallpox vaccinee. *Clin Infect Dis* 2008; **46**: 1555–61.

37 Lederman ER, Davidson W, Groff HL *et al*. Progressive vaccinia: case description and laboratory-guided therapy with vaccinia immune globulin, ST-246, and CMX001. *J Infect Dis* 2012; **206**: 1372–85.

38 Chen Y, Honeychurch KM, Yang G *et al*. Vaccinia virus p37 interacts with host proteins associated with LE-derived transport vesicle biogenesis. *Virol J* 2009; **6**: 44.

39 Smith GL. Genus *Orthopoxvirus*: vaccinia virus. In: Mercer AA, Schmidt A, Weber O, eds. *Poxviruses*. Basel: Birkhäuser, 2007; 1–45.

40 Blasco R, Moss B. Extracellular vaccinia virus formation and cell-to-cell virus transmission are prevented by deletion of the gene encoding the 37,000-Dalton outer envelope protein. *J Virol* 1991; **65**: 5910–20.

41 Vliegen I, Yang G, Hruby D *et al*. Deletion of the vaccinia virus F13L gene results in a highly attenuated virus that mounts a protective immune response against subsequent vaccinia virus challenge. *Antiviral Res* 2012; **93**: 160–6.

42 Grosenbach DW, Ulaeto DO, Hruby DE. Palmitylation of the vaccinia virus 37-kDa major envelope antigen. Identification of a conserved acceptor motif and biological relevance. *J Biol Chem* 1997; **272**: 1956–64.

43 Roper RL, Moss B. Envelope formation is blocked by mutation of a sequence related to the HKD phospholipid metabolism motif in the vaccinia virus F13L protein. *J Virol* 1999; **73**: 1108–17.

44 Schmutz C, Payne LG, Gubser J *et al*. A mutation in the gene encoding the vaccinia virus 37,000-M_r protein confers resistance to an inhibitor of virus envelopment and release. *J Virol* 1991; **65**: 3435–42.

45 Isaacs SN, Wolffe EJ, Payne LG *et al*. Characterization of a vaccinia virus-encoded 42-kilodalton class I membrane glycoprotein component of the extracellular virus envelope. *J Virol* 1992; **66**: 7217–24.

46 Engelstad M, Smith GL. The vaccinia virus 42-kDa envelope protein is required for the envelopment and egress of extracellular virus and for virus virulence. *Virology* 1993; **194**: 627–37.

47 Husain M, Moss B. Vaccinia virus F13L protein with a conserved phospholipase catalytic motif induces colocalization of the B5R envelope glycoprotein in post-Golgi vesicles. *J Virol* 2001; **75**: 7528–42.

48 Payne LG. Characterization of vaccinia virus glycoproteins by monoclonal antibody precipitation. *Virology* 1992; **187**: 251–60.

49 Duraffour S, Vigne S, Vermeire K *et al*. Specific targeting of the F13L protein by ST-246 affects orthopoxvirus production differently. *Antivir Ther* 2008; **13**: 977–90.

50 Lorenzo MM, Sanchez-Puig JM, Blasco R. Mutagenesis of the palmitoylation site in vaccinia virus envelope glycoprotein B5. *J Gen Virol* 2012; **93**: 733–43.

51 Duraffour S, Andrei G, Topalis D *et al*. Mutations conferring resistance to viral DNA polymerase inhibitors in camelpox virus give different drug-susceptibility profiles in vaccinia virus. *J Virol* 2012; **86**: 7310–25.

52 Lorenzo MM, Galindo I, Blasco R. Construction and isolation of recombinant vaccinia virus using genetic markers. *Methods Mol Biol* 2004; **269**: 15–30.

53 Duraffour S, Mertens B, Meyer H *et al*. Emergence of cowpox: study of the virulence of clinical strains and evaluation of antivirals. *PLoS One* 2013; **8**: e55808.

54 Arnold K, Bordoli L, Kopp J *et al*. The SWISS-MODEL workspace: a web-based environment for protein structure homology modelling. *Bioinformatics* 2006; **22**: 195–201.

55 Bordoli L, Kiefer F, Arnold K *et al*. Protein structure homology modeling using SWISS-MODEL workspace. *Nat Protoc* 2009; **4**: 1–13.

56 Leiros I, McSweeney S, Hough E. The reaction mechanism of phospholipase D from *Streptomyces* sp. strain PMF. Snapshots along the reaction pathway reveal a pentacoordinate reaction intermediate and an unexpected final product. *J Mol Biol* 2004; **339**: 805–20.

57 Benkert P, Biasini M, Schwede T. Toward the estimation of the absolute quality of individual protein structure models. *Bioinformatics* 2011; **27**: 343–50.

58 Kelley LA, Sternberg MJ. Protein structure prediction on the Web: a case study using the Phyre server. *Nat Protoc* 2009; **4**: 363–71.

59 Kallberg M, Wang H, Wang S *et al*. Template-based protein structure modeling using the RaptorX web server. *Nat Protoc* 2012; **7**: 1511–22.

60 Smith GL, Vanderplasschen A, Law M. The formation and function of extracellular enveloped vaccinia virus. *J Gen Virol* 2002; **83**: 2915–31.

61 Herrera E, Lorenzo MM, Blasco R *et al*. Functional analysis of vaccinia virus B5R protein: essential role in virus envelopment is independent of a large portion of the extracellular domain. *J Virol* 1998; **72**: 294–302.

62 Lorenzo MM, Galindo I, Griffiths G *et al*. Intracellular localization of vaccinia virus extracellular enveloped virus envelope proteins individually expressed using a Semliki Forest virus replicon. *J Virol* 2000; **74**: 10535–50.

63 Husain M, Moss B. Similarities in the induction of post-Golgi vesicles by the vaccinia virus F13L protein and phospholipase D. *J Virol* 2002; **76**: 7777–89.

64 Carroll DS, Emerson GL, Li Y *et al*. Chasing Jenner's vaccine: revisiting cowpox virus classification. *PLoS One* 2011; **6**: e23086.

65 Quenelle DC, Kern ER. Treatment of vaccinia and cowpox virus infections in mice with CMX001 and ST-246. *Viruses* 2010; **2**: 2681–95.

66 Blasco R, Moss B. Role of cell-associated enveloped vaccinia virus in cell-to-cell spread. *J Virol* 1992; **66**: 4170–9.

67 Baek SH, Kwak JY, Lee SH *et al*. Lipase activities of p37, the major envelope protein of vaccinia virus. *J Biol Chem* 1997; **272**: 32042–9.